WELDER•SVÁŘEČ•SCHWEISSER•СВАРЩИК•SOUDEUR•SPAWACZ•SALDATORE•HEGESZTŐ•ZAVARIVAČ

ZVÁRAČ

profesionál

ROČNÍK XVIII 2021 3

AKTUALITY ZO SVETA ZVÁRANIA, SPÁJKOVANIA A DELIACICH TECHNOLÓGIÍ

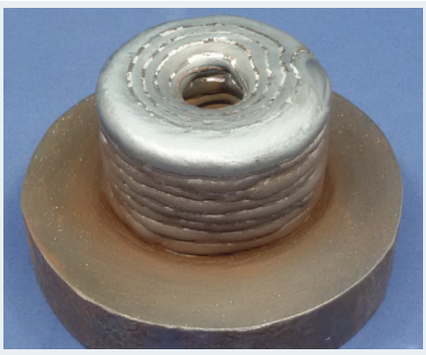

P. Gröninger, F. Koch, G. Trensch, S. Keitel

Contribution to the heat management in Wire Arc Additive Manufacturing with gas flow based cooling strategies

This work examines the possibilities to reduce the cooling time for the Wire Arc Additive Manufacturing (WAAM) process. The WAAM generates near-net-shape metal objects. During the build-up process...

str. 3

Arc-Eye CSS Adaptive Welding

Běžný svařovací robot jednoduše dělá to, co se naučil, a jako svářeč se nedívá na samotnou skutečnou situaci. Pokud vybavíme robota systémem sledování svarové spáry, jako je laserová kamera Arc-Eye CSS, robot dokáže dokonale detekovat odchylky polohy svaru a upravit trajektorii robota v reálném čase. Stejně tak ruční...

str. 29

Separačný prostriedok so štandardom NF. Super Pistolenspray NF

Tento nadpriemerne účinný sprej je skutočne všestranný, pretože je vhodný na ošetrenie plynovej hubice/dýzy, ale aj na obrobok a upínacie prvky. Rozstrek zo zvaru sa nemá šancu natrvalo pripáliť a dá sa následne ľahko odstrániť.

str. 34

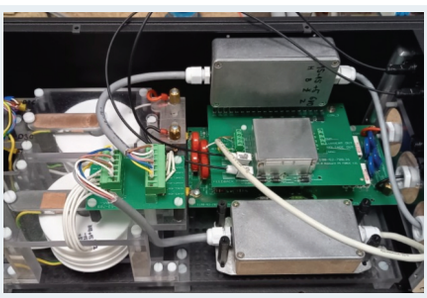

R. Sekerka, F. Kolenič, M. Brdečka, P. Koršnák, D. Kunštek

Regulácia zvlnenia zváracieho prúdu pomocou napäťového zdroja ohrevu katódy

Príspevok prezentuje riešenie topológie modulu regulácie striedavej zložky zváracieho prúdu pri zváraní elektrónovým lúčom. Je popísaný dizajn napäťového zdroja ohrevu katódy, ktorý umožňuje formovať časový priebeh zváracieho prúdu pri elektrónovolúčovom zváraní. Striedavý signál, ktorým je modulovaná...

str. 9

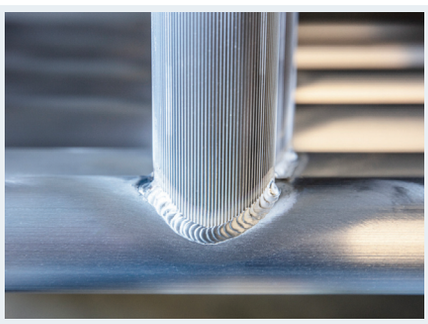

Ľahké priemyselné konštrukcie z hliníka: riešenia prístupu od spoločnosti ALTEC

Montáže lešení najrôznejšieho druhu, ako napríklad dokovacie zariadenia pre lietadlá: riešenia prístupu od spoločnosti ALTEC sa zhotovujú prevažne z hliníka. Spoločnosť sa pritom spolieha na zváraciu techniku od Froniusu. Vďaka zváraciemu postupu CMT, ako aj pulznej charakteristike Rippledrive nastavila spoločnosť...

str. 30

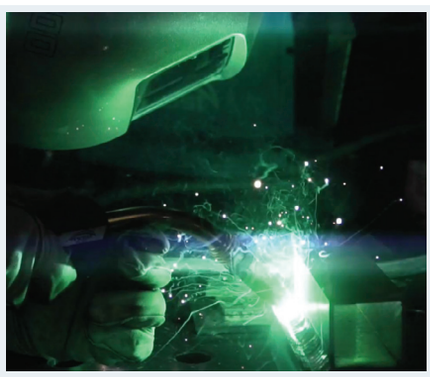

Pulzná invertorová zváračka Fanmig J5 Pulse – zváranie bez rozstreku

Najpredávanejšiu zváračku značky MOST doplnila pulzná technológia. Na trhu sa tak objavila novinka – Fanmig J5 Pulse na pulzné zváranie hliníka, nerezu a ocele. Model Fanmig J5 je u našich zákazníkov veľmi obľúbený, preto sme sa nevedeli dočkať testovania...

str. 39

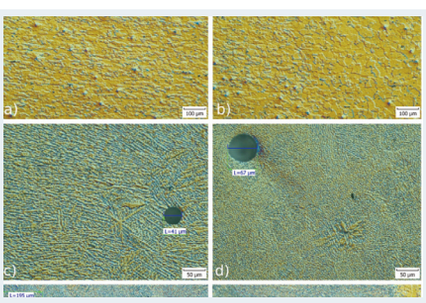

M. Vyskoč

Vplyv ochranných plynov na pórovitosť laserových zvarových spojov z hliníkovej zliatiny AW 5083

Príspevok sa zaoberá hodnotením vplyvu ochranných plynov na vlastnosti zvarových spojov z hliníkovej zliatiny AW 5083 vyhotovených diskovým laserom. Tupé zvarové spoje boli vyhotovené pri rôznych druhoch ochranných plynov, konkrétne Ar 4.6, He 4.6, Ar + 5 obj. % He, Ar + 30 obj. He. Na hodnotenie vlastností...

str. 15

QINEO StarT– jednoduše lepší svařování

Svařovací zdroj konstrukční řady QINEO StarT (MIG/MAG) Vám díky své všestrannosti vždy nabídne správné řešení vašeho individuálního svařovacího úkolu - ruční nebo automatizované svařování, tenkostěnné nebo silnostěnné materiály, které vyžadují speciální...

str. 32

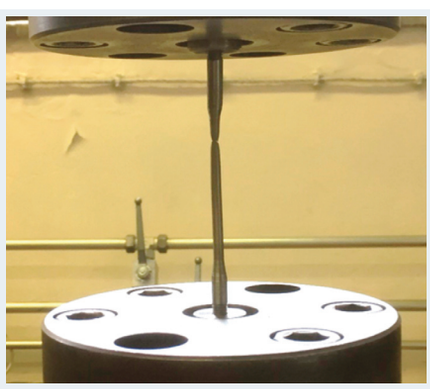

Využitie spektrometrie pri posudzovaní zvarových spojov po viacročnej prevádzke

Posúdenie aktuálneho stavu konštrukcie a jej prevádzkyschopnosti po niekoľkých desaťročiach činnosti je náročná úloha, ktorá vyžaduje identifikáciu materiálu a jeho chemického zloženia, znalosť aktuálnych...

str. 43

Contribution to the heat management in Wire Arc Additive Manufacturing with gas flow based cooling strategies

Príspevok k tepelnému manažmentu pri oblúkovej aditívnej výrobe s využitím variantných riešení chladenia prietokom plynu




Philipp Gröninger[1]
Dr.-Ing. Felix Koch[1]
Georg Trensch[1]
Prof. Dr.-Ing. Steffen Keitel[2]

Research and Development, SLV Halle GmbH/ Germany, Köthener Str. 33a, 06118 Halle (Saale)
[1]Research and Development, SLV Halle GmbH
[2]CEO, Head of Department Research and Development, SLV Halle GmbH

e-mail: groeninger@slv-halle.de, felixkoch@slv-halle.de, trensch@slv-halle.de, keitel@slv-halle.de

Tento vedecký článok recenzoval: Ing. František Kolenič, PhD.

This work examines the possibilities to reduce the cooling time for the Wire Arc Additive Manufacturing (WAAM) process. The WAAM generates near-net-shape metal objects. During the build-up process the heat transfer conditions are changing which results in excessive heat accumulation. The heat is controlled by pausing the build-up process in which the object is cooled down to a predefined temperature. To examine the most effective way to reduce this non-productive time a water-cooled base table, a vortex tube, an air amplifier, and a CO_2-cooling system are compared with each other. With the purpose of assessing the heat dissipation, the temperature is recorded during the build-up and cooling process with an infrared camera and thermocouple elements. This leads to the conclusion that the effectiveness of the three used cooling systems depends on the geometry of the object. The rate of volume to surface determines the cooling down speed. Furthermore, the option of reducing the heat input through changing the tool path generation strategy and the characteristic curve are examined. The results show that the cooling time depends on many different elements and thus can be reduced in different phases of the whole process.

Predložený príspevok skúma možnosti skrátenia času chladenia pri procese aditívnej výroby kovových objektov pomocou oblúkových technológií s prídavným materiálom vo forme drôtu (WAAM). Metóda WAAM umožňuje vytvárať 3D kovové objekty takmer nahotovo. Počas procesu výroby objektu sa menia podmienky prenosu tepla, čo má za následok nadmerné hromadenie tepla v objekte a prekročenie kritickej teploty. V rámci realizovaných experimentov bolo množstvo dodávaného tepla regulované pozastavením procesu aditívnej výroby na určitý čas. V čase pozastavenia procesu zvárania sa nadbytočné teplo odvádzalo z objektu ochladením na vopred definovanú teplotu. Boli skúmané tri spôsoby chladenia výrobku počas odstávky zvárania. Chladenie bolo realizované pomocou vírivej trubice, vzduchového zosilňovača a systému chladenia pomocou CO_2. Na účely posúdenia rozptylu tepla a účinnosti chladenia bola počas procesu aditívnej výroby zaznamenávaná teplota výrobku infračervenou kamerou a termočlánkami. Dosiahnuté výsledky vedú k záveru, že účinnosť troch skúmaných spôsobov chladenia závisí v hlavnej miere od geometrie vytváraného objektu. Bola skúmaná aj možnosť zníženia prívodu tepla zmenou trajektórie navárania. Výsledky ukazujú, že doba chladenia objektu počas odstávky aditívneho procesu závisí od mnohých faktorov a môže byť efektívne skrátená v rôznych fázach procesu aditívnej výroby.

1. INTRODUCTION

Since Chuck Hull applied the first 3D-print technology for patent in 1986 a broad area of applications has developed. Today 3D printing consists of Rapid Prototyping (RP), Rapid Tooling (RT), Rapid Manufacturing (RM) and Rapid Repair RR) [1]. Furthermore, 3D printing can be classified into seven different process categories. Yet it is only possible to manufacture metal with directed energy deposition (DED) and powder bed fusion (PBF) [2]. According to the source of energy DED can be separated into laser-based, electron beam-based and arc welding-based [3]. Wire Arc Additive Manufacturing (WAAM) is an arc welding-based process. The advantage of the WAAM compared to the laser-based and the electron beam-based processes is the high energy efficiency and deposition rate and the more economical equipment [4]. The high deposition rate is achieved through a high energy input. During the build-up process the heat transfer conditions are changing which results in excessive heat accumulation. The outcome is an instable and changing deposit after each layer [5]. According to Yang [6] the heat accumulation can be managed through inter-layer cooling time. This research shows that a longer inter-layer cooling-time reduces the mean temperature and increases the surface smoothness, which is the result of a stable deposit. The disadvantage of inter-layer cooling-times is, that in order to manage the heat the length of the inter-layer cooling time has to be determined for each structure individually. Furthermore, the cooling times are non-productive-times. To keep the process economical and to be able to compete with conventional processes the non-productive

time has to be reduced. A solution is the interpass temperature control and active cooling. The interpass temperature control stops the deposition after each layer till the temperature in the last deposited layer drops below the predefined temperature. Kozamernik [7] concludes that the interpass temperature control is critical to achieve repeatable and stable deposition height throughout the layers and that active air cooling improves the productivity by up to 30 %. Reisgen [8] made a further step in his research and compared advanced cooling strategies with each other. The result shows that the water bath cooling method has the highest cooling effect followed by aerosol cooling and high-pressure air cooling. Though the gas flow based cooling strategies are not the most effective in terms of the cooling effect they offer a higher degree of freedom for the manufacturing process and are less complicated to implement than water bath cooling. Thus, this paper concentrates on finding ways to maximize the cooling effect of gas flow based cooling strategies and to reduce the cooling time during the WAAM-process.

2. EXPERIMENTAL PROCEDURE

2.1 Experimental system

The experiments are performed on the arc405 system designed by the company Gefertec. The arc405 system is a WAAM machine which contains the Fronius synergic 4000 power supply and a fume extractor. A portal frame CNC machine is used to move the torch in all three directions (axes). In addition, the table can be rotated and tilted. The total of five axes allows the generation of overhanging structures without support. To keep the temperature manageable the table of the arc405 is water cooled. For the interpass temperature control the arc405 is equipped with a built-in pyrometer "Metis M318" and an air amplifier Airmasters40 for active cooling (Figure 1). Additionally, a vortex tube and a carbon dioxide cooling system are used for active cooling. Through a subprogram the flow of the high-pressure air is started and stopped with the beginning and end of the interpass temperature control. The flow of the carbon dioxide is started and stopped manually by a switch. To assess the heat dissipation, the temperature is recorded with the infrared camera "Optris PI 640" and with thermocouple elements type K.

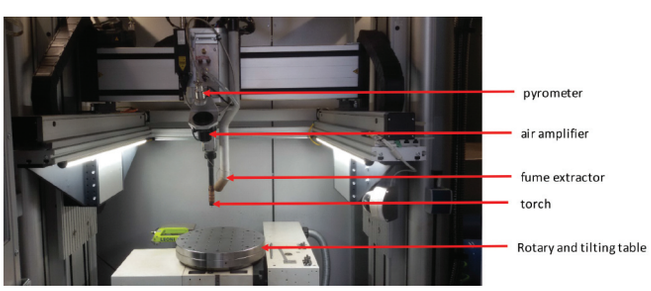

Fig. 1 Structure of the arc405
Obr. 1. Experimentálne pracovisko arc405

2.2 Arrangement of the experiments

A lot of research on this topic has been carried out focusing on thin walls. Since most structures consist of more than just one weld bead a hollow cylinder with an outside diameter of 50 mm and an inside diameter of 15 mm is used (Figure 2). For the build-up process the wire WDI 15 SG with the standard designation DIN EN ISO 14341-A and 1.2 mm diameter is used on a mild steel plate with a diameter of 90 mm and a thickness of 15 mm. The shielding gas for the torch is M12 (Ar + 2.5% $CO_{2)}$ with a constant flow rate of 15 l/min. Three different gas flow cooling strategies are conducted, high pressure air amplified by the Airmasters40 or by the vortex tube and carbon dioxide released through a nozzle. In each of the experiments the structure is built layer by layer. The interpass temperature control is executed after every second layer. The first experiment is done without any cooling, the second with the Airmasters40, the third with the vortex tube and the fourth with carbon dioxide. The interpass temperature is set to 150 °C. The time in which the interpass temperature control is active is recorded to evaluate the cooling times. Furthermore, the temperature profile of the structure is recorded during the whole build-up process with the help of the infrared camera. In addition, the temperature in the mild steel plate is recorded with thermocouple elements. The mild steel plate is clamped inside a jig in a distance of 150 mm to the water cooled table. This ensures that the water cooled table has no effect on the cooling process and only the gas flow based cooling strategies are taken into account.

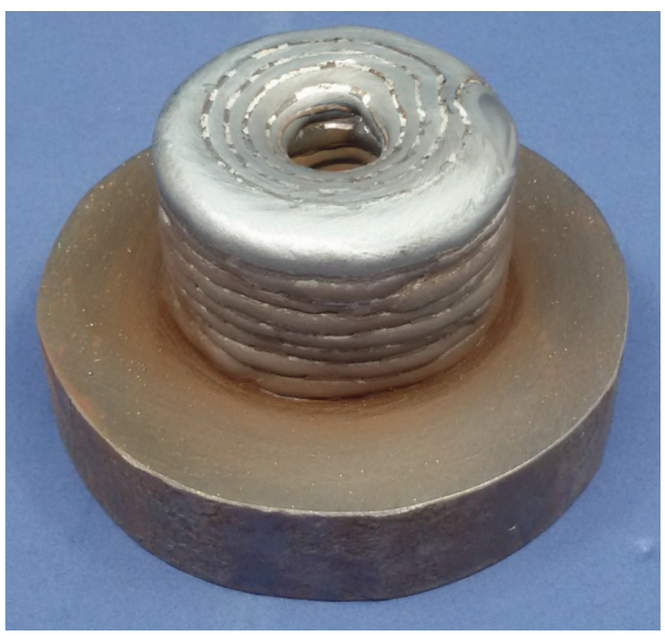

Fig. 2 Hollow cylinder produced by WAAM process
Obr. 2. Dutý valec vyrobený procesom WAAM

3. Forced convection heat transfer

The heat dissipation caused by gas flow based cooling strategies is the result of forced convection. The rate of convection heat transfer Q is a function of the surface area A where the heat transfer takes place, the difference in temperature between the solid surface and surrounding fluid ΔT and the heat transfer coefficient h (see equation (1)) [9].

$$\dot{Q} = h \cdot \Delta T \cdot A \qquad (1)$$

In order to increase the rate of the heat convection the three variables A,ΔT and h have to be raised. The surface area is defined by the structure of the part and thus can only be influenced through the design. By using a gas with a low temperature compared to the solid surface, the heat convection can be raised and thus the cooling time decreased. Another way to do so is to increase the heat transfer coefficient. The heat transfer coefficient is a function of the thermal conductivity k, the mean Nusselt number Nu_m and the characteristic length L' (see equation (2)) [9]. Thus, it depends on correlations for particular geometry and flow conditions. Equation 2 shows that the

heat transfer coefficient is can be influenced by the flow rate (Num) and of material-dependent variables (k,Nu_m).

$$\alpha = \frac{k * Nu_m}{L'} \quad (2)$$

These variables depend on the temperature and the pressure of the gas [9]. Figure 3a) shows the heat transfer coefficient in dependency of flow rate and temperature and figure 3b) shows the dependency to flow rate and pressure. As seen in figure 3 the pressure raises the heat transfer coefficient h most efficiently followed by the flow rate and the temperature. Since it is difficult to raise the pressure of the gas a more economical way to increase the heat transfer coefficient and to reduce the cooling time is to increase the flow rate. Therefore, nozzles for each of the cooling strategies were designed.

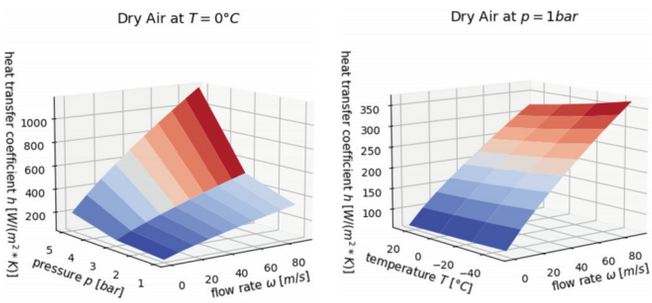

Fig. 3 heat transfer coefficient in dependency of flow rate and a) pressure b) temperature
Obr. 3. Koeficient prestupu tepla v závislosti od (a) prietoku a tlaku, (b) prietoku a teploty

Another way to increase the heat transfer coefficient is to change to a gas with increased heat conductivity characteristics. Figure 4 compares the heat transfer coefficient of three different gases. The result is that the heat transfer coefficient can be raised by selecting a different gas.

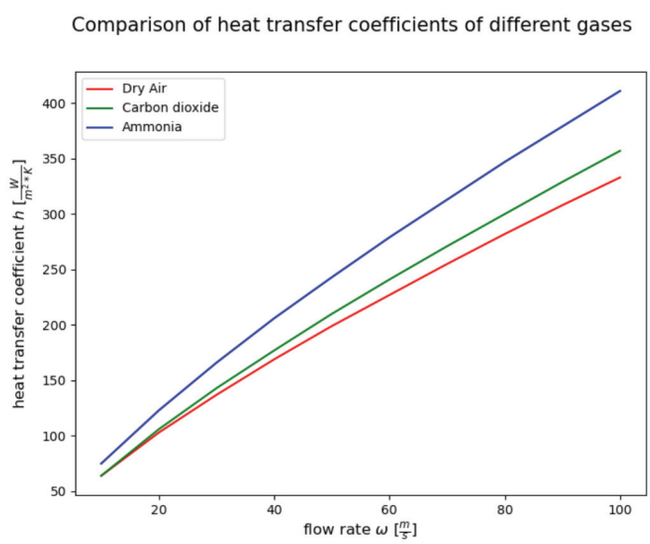

Fig. 4 Comparison of heat transfer coefficients of different gases
Obr. 4. Porovnanie koeficientov prestupu tepla rôznych plynov

The setup of the three cooling strategies is done according to this overview. Table 1 states the parameter of each cooling strategy.

Tab. 1 Parameters of the cooling strategies
Tab. 1. Parametre variantných spôsobov chladenia

Cooling strategy	Temperature [°C]	Flow rate [m/s]	Pressure [bar]
Airmasters40	25	20	1
Vortex tube	20	53	1
Carbon dioxide cooling	0	56	1

4. RESULTS AND DISCUSSION

4.1 Cooling times

In table 2 the cooling times of the different cooling strategies are listed. Compared to the cooling time without any active cooling all cooling strategies are a huge improvement in terms of the cooling times and thus economically. The most effective way of cooling is carbon dioxide cooling with a total cooling time of 663.5 s followed by the vortex tube with 819.8 s and the Airmasters40 with 1309.4 s. The cooling times after each two layers are almost identical which confirms a constant heat input and heat transfer. The cooling times only differ if the second layer is compared with the fourth layer, except for the vortex tubes. This can be explained with the cold steel plate and jig. Through heat conduction the heat is proportionately transferred from the structure. Since the dimension of the steel plate are small this effect stops after the fourth layer. This leads to the conclusion that if the structure is generated on steel plates with large dimensions it will reduce the cooling time up to a certain layer. This effect cannot be observed at the vortex tube due to the narrow air nozzle which is directed mostly at the upper layers. Because of this, the cooling effect for the first two layers is cause by the cold steel plate rather than the vortex tube so that the cooling time remains constant.

Tab. 2 Cooling times of the different cooling strategies
Tab. 2. Časy chladenia v závislosti od spôsobov chladenia

Cooling strategy	none	Airmasters40	Vortex tube	Carbon dioxide cooling
Current I [A]	138.0	138.0	138.0	138.0
Voltage U [V]	14.0	14.0	14.0	14.0
t_manufacturing [s]	608.5	608.5	608.5	608.5
t_cooling [s] layer 2	817.4	308.7	207.2	153.1
t_cooling [s] layer 4	858.1	330.3	208.9	168.6
t_cooling [s] layer 6	861.8	335.6	202.2	170.4
t_cooling [s] layer 8	865.3	334.8	201.5	171.4
t_cooling_total [s]	3402.6	1309.4	819.8	663.5

In figure 5 the cooling times and the heat transfer coefficient (calculated with equation 1 and 2 and with the parameters out of table 1) are displayed. The reduction of the cooling time of around 37 % results in a steeper rise of the heat transfer coefficient, than the reduction of the cooling time from 37% to 49%. This leads to the conclusion that a coherence exists between the cooling time and the heat transfer coefficient. To be able to roughly predict the cooling time for any cooling strategy this coherence has to be expressed in an equation.

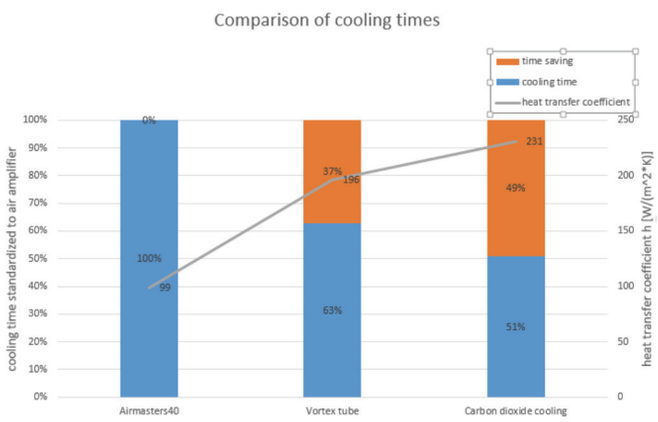

Fig. 5 Comparison of the cooling times and the corresponding heat transfer coefficients
Obr. 5. Porovnanie časov chladenia a zodpovedajúcich koeficientov prestupu tepla

If the temperature of the cooling gas of two different cooling strategies is not the same, the cooling time is not only influenced by the heat transfer coefficient as shown in figure 5, but it is a function of the rate of convection heat transfer. The cooling time of a new cooling strategy ($t_{cooling_{new}}$) can be roughly calculated with the rate of the convection heat transfer of the new cooling strategy ($\dot{Q}_{new}$), of the available cooling strategy ($\dot{Q}_{available}$) and the cooling time of the available cooling strategy ($t_{cooling_{available}}$) (see equation (3)). $\dot{Q}_{new}$ and $\dot{Q}_{available}$ have to be calculated theoretically and $t_{cooling_{available}}$ is determined experimentally. Equation 3 was founded based on experiments with different cooling strategies. The equation only applies if a reference cooling system exits, which is labeled “available” here.

$$t_{cooling_{new}} = \left(\frac{\dot{Q}_{new}}{\dot{Q}_{available}} + 0.12 \right) \cdot t_{cooling_{available}} \qquad (3)$$

Equation 3 provides only a rough calculation for the expected time. It is based on a certain geometry which was generated with certain parameters. If generally applied the results will differ, but the equation indicates how the new cooling strategy will affect the cooling time. In order to apply the equation, the parameters of the gas such as temperature, flow rate and pressure have to be known.

4.2 Recording the temperature with thermocouple elements

In order to understand the cooling process better it is necessary to understand how the temperature evolves during the buildup process. To get a realistic picture of the temperature the buildup process is not stopped in between to add further thermocouple elements. So, the temperature is recorded on the mild steel plate at four different points, all of them 90 ° steps apart from each other (figure 6). This allows the observation of the temperature profile by direct heat input on the mild steel plate for the first layers. For the later layers, there is a growing distance between the heat input and the measurement points.

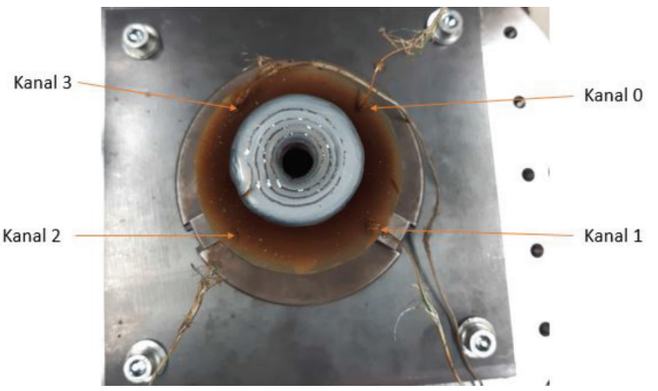

Fig. 6 Arrangement of the thermocouple elements
Obr. 6. Usporiadanie termočlánkov pri meraní teploty objektu

Figure 7 shows the temperature profile over the whole buildup process cooled active in a) with the Airmasters40 and b) with the vortex tube. The four colored lines represent the four different thermocouple elements. The temperature at the four points do almost not differ from each other. This shows that the temperature transfer evens within the mild steel plate. The time when the graphs are rising is the time when the torch is on. Afterwards comes the cooling time in which the temperature falls. Eight layers are recorded. The blips in the graphs are created through the circulate movement of the torch. Every turn the torch passes each of the thermocouple elements on time. With the continuous processing of the layer the torch passes the thermocouple elements always a bit closer so that the blips become more distinct. At the peak the blips are the highest. This is because in the last turn of the layer the plasma flare sideslips

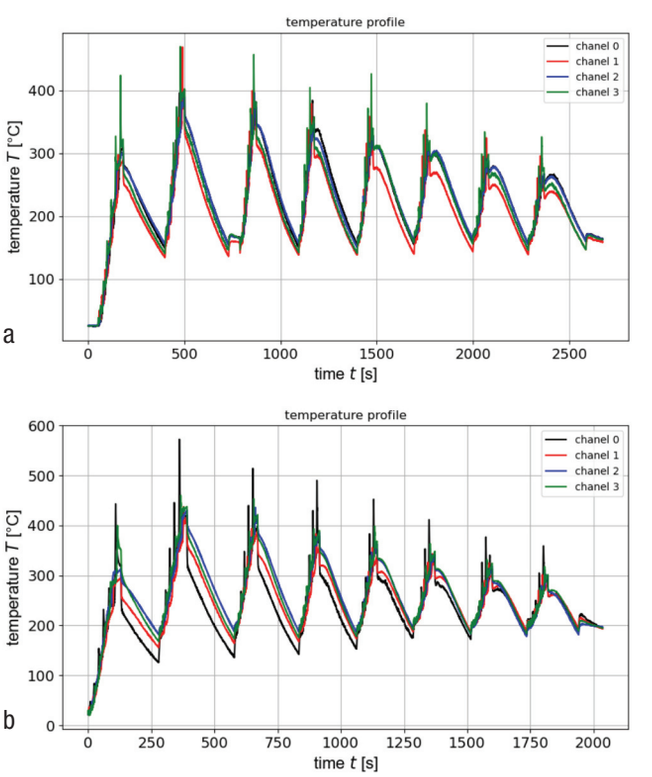

Fig. 7 Temperature profile over the whole buildup process with a) Airmasters40 b) vortex tube
Obr. 7 Teplotný profil výrobku počas celého procesu aditívnej výroby
a) chladenie systémom Airmasters40, b) chladenie pomocou vortexovej trubice

and hits the mild steel plate and the thermocouple elements on it. Due to this the temperature rises suddenly and once the plasma flare has passed it drops again. The manufacturing time with the vortex tube cooling (figure 7b) is compared to the Airmasters40 (figure 7a) cooling over 500 s faster. The interpass temperature in both experiments is 150 °C. In figure 7a this temperature is always reached in the mild steel plate. In figure 7b this is not the case. This indicates a more efficient cooling process. The air flow of both cooling systems is directed on the last manufactured layer. The pyrometer is also directed there. So, when the interpass temperature is reached in the last manufactured layer the buildup process continues. If the cooling is not effective enough the heat has time to spread evenly through the whole part due to heat conduction. The advantage is that the peak temperatures are lower than with the vortex tube cooling (figure 5b). The peak temperature in both cases is decreasing after every layer. The reason for it is the increasing distance between the thermocouple elements and the heat input. After a certain amount of layers, the temperature will level off at about the interpass temperature and stay constant there. Figure 7 shows that especially in the last layer the temperature does not drop directly after the torch is turned off, but that it stays on a plateau or even rises again.

This is an unusual cooling down process. To analyse the rising of the temperature in the cooling down phase the temperature is differentiated with respect to the time. The result is a temperature gradient. In figure 8 the temperature gradient is shown in the first and the last layer with Airmasters40 cooling. A positive temperature gradient means the part is heating up and a negative one means it is cooling down. Normally when a part cools down the temperature drops faster in the beginning and slows down towards the aim temperature. Thus, the temperature gradient should be the highest at the start of the cooling process and then continuously decrease. In figure 8a the temperature gradient is close to what is expected. In figure 8b the temperature gradient becomes positive. This means that the mild steel plate is heated up despite the cooling down phase with active cooling of the last generated. This is against the first law of the thermodynamics which states that the total energy of an isolated system is constant. This means that a body cannot heat itself up without an external heat input. This is in contradiction to the rising of the temperature in the mild steel plate. The heating up of the steel plate indicates insufficient cooling. The heat which is brought into the part by the torch cannot be adequately transferred from the part by convection. The second law of thermodynamics states that heat can never pass from a colder to a warm body without any other changes. If the cooling is not sufficient enough the heat is transferred into the mild steel plate through heat conduction. This causes the heat to stay longer inside the part and the cooling time goes up.

The vortex tube cools more efficiently than the Airmasters40. If this conclusion is true the temperature gradient of the vortex tube cooling should show a more normal trend than the one from the Airmasters40. Figure 9 shows that the cooling is still not sufficient since 3 of the 4 channels still show a positive temperature gradient. Compared to figure 8b the trend in figure 9 is closer to a normal trend. This confirms that the conclusion is right.

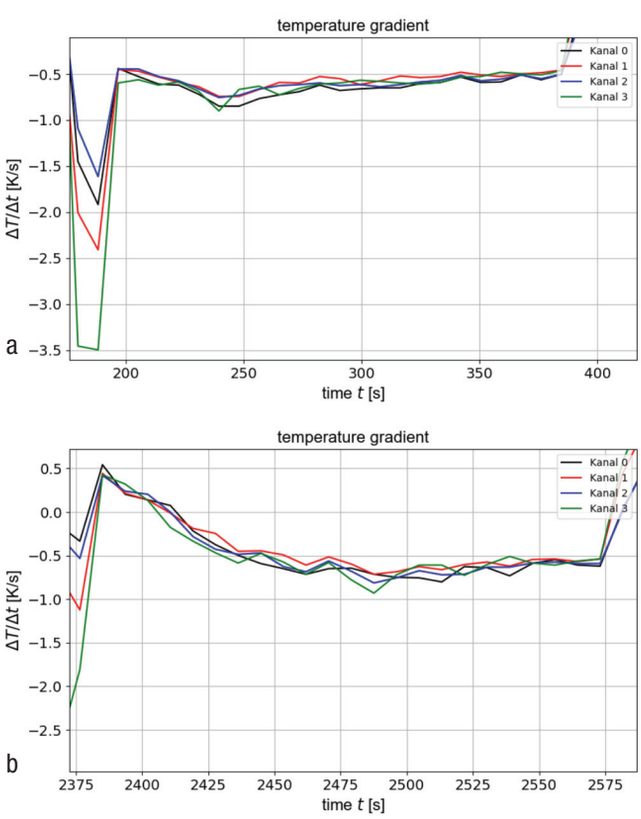

Fig. 8 Temperature gradient with Airmasters40 cooling in a) the first layer b) the eights layer

Obr. 8. Teplotný gradient s chladením Airmasters40 a) v prvej vrstve, b) v ôsmej vrstve

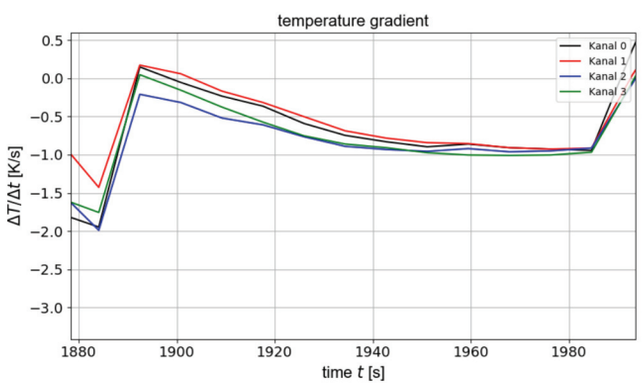

Fig. 9 Temperature gradient with vortex tube in the eights layer

Obr. 9. Teplotný gradient s vírivou trubicou vortex v ôsmej vrstve

4.3 Recording the temperature with an infrared camera

The recording of the temperature with the thermocouple elements only shows the temperature profile at the mild steel plate. With the infrared camera the temperature profile of the whole part can be assessed. The temperature is recorded for the whole build up process with Airmasters40 cooling and vortex tube cooling. To be able to manage the data the temperatures at 3 points as shown in figure 10 are recorded.

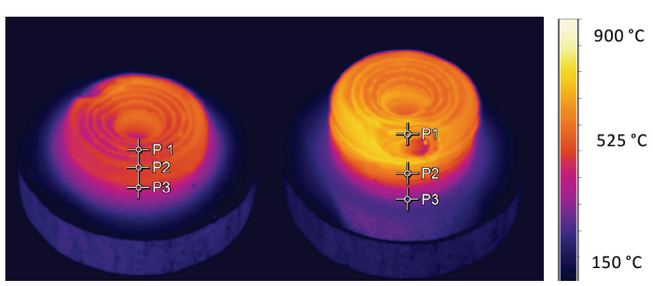

Fig. 10 Arrangement of the three measurement points after a) the fourth layer b) the eights layer

Obr. 10. Usporiadanie troch meracích bodov a) po štvrtej vrstve, b) po ôsmej vrstve

Figure 11 shows the temperature profile after the fourth and the eighths layer. The dashed line marks the point when the active cooling process starts. On the left of the dashed line the torch is on. The undulated shape of the graph comes from the circulate movement of the torch. The temperatures in the three points are closer to each other after the fourth layer than after the eighths layer. The heat transfer through heat conduction inside the part decreases with growing distance of the points to each other. The heat input of the torch only influences the layers directly located under the ones just created. When the cooling is switched on the temperature drops more quickly. Figure 11 also shows that the air flow is directed on the last generated layer because the temperature from point 1 and 2 falls below the temperature at point 3. The temperature profile shows that active cooling and the interpass temperature control is crucial to manage the heat inside the part.

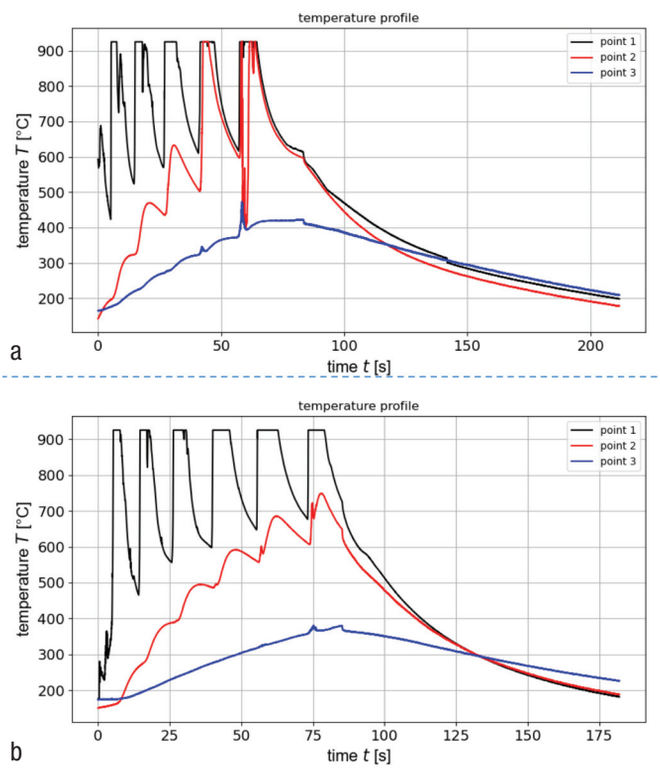

Fig. 11 Temperature profile after a) the fourth layer b) after the eighths layer

Obr. 11. Teplotný profil po a) štvrtej vrstve, b) po ôsmej vrstve

5. Conclusion

Based on the presented work the following statements can be made.

- Gas flow based cooling strategies cool more effectively if used at low temperature, with a high flow rate and under pressure.
- The decrease of the flow rate to around 60 % reduces the cooling time to around 37 %.
- If the fluid is changed from air to carbon dioxide and the temperature is dropped to around 40 K the cooling time is reduced by approximately another 19 %.
- The cooling time can be approximately calculated for another cooling strategies if the parameters like flow rate etc. are known.
- Insufficient cooling leads to heat transfer within the part. The heat stays inside the part and the cooling time is prolonged.
- A directed gas flow on the last generated layer leads to a higher heading up of the part, since the buildup process continues once the interpass temperature is reached in the last generated layer.
- The higher the part grows, the more slowly the heat is transferred to the first generated layers.

Further steps will contain the investigation about the influence of the cooling rate on the microstructure evolution. Finally, the cooling strategies have to be compared with regard to the particular workpiece geometry by economical aspects.

REFERENCES:

[1] Roland Lachmayer, Rene Bastian Lippert, Thomas Fahlbusch, title: 3D-Druck beleuchtet: Additive Manufacturing auf dem Weg in die Anwendung, Verlag: Springer Vieweg, ISBN: 978-3-662-49055-6

[2] DIN EN ISO /ASTM 52900:2018

[3] Ding, D., Pan, Z., Cuiuri, D. et al. Wire-feed additive manufacturing of metal components: technologies, developments and future interests. Int J Adv Manuf Technol 81, 465–481 (2015). https://doi.org/10.1007/s00170-015-7077-3

[4] Hassel, T., Carstensen, T. Properties and anisotropy behaviour of nickel base alloy material produced by robot-based wire and arc additive manufacturing. Welding in the World 64, 1921-1931 (2020). https://doi.org/10.1007/s40194-020-00971-7

[5] Bai X, Zhang H, Wang G. Improving prediction accuracy of thermal analysis for weld-based additive manufacturing by calibrating input parameters using IR imaging. Int J Adv Manuf Technol 69, 1087–1095 (2013) https://doi.org/10.1007/s00170-013-5102-y

[6] Yang, D., Wang, G., Zhang, G. Thermal analysis for single-pass multi-layer GNAW based additive manufacturing using infrared thermography. Journal of Material Processing Technology 244, 215-224 (2017)

[7] Kozamernik, N., Bracun, D., Klobcar, D. WAAM system with interpass temperature control and forced cooling for neat-net-shape printing of small metal components. The International Journal of Advanced Manufacturing Technology 110, 1955-1968 (2020). https://doi.org/10.1007/s00170-020-05958-8

[8] Reisgen, U., Sharma, R., Mann, S., Oster, L. Increasing the manufacturing efficiency of WAAM by advanced cooling strategies. Wlding in the World 64, 1409-1416 (2020), https://doi.org/10.1007/s40194-020-00930-2

[9] Gnielinski V. (2019) G6 Wärmeübertragung bei erzwungener Konvektion: Querumströmte einzelne Rohre, Drähte und Profilzylinder. In: Stephan P., Kabelac S., Kind M., Mewes D., Schaber K., Wetzel T. (eds) VDI-Wärmeatlas. Springer Reference Technik (VDI Springer Reference). Springer Vieweg, Berlin, Heidelberg. https://doi.org/10.1007/978-3-662-52989-8_47